JACS
JOURNAL OF THE AMERICAN CHEMICAL SOCIETY
Communication
pubs.acs.org/JACS

The Chemistry of CO_2 Capture in an Amine-Functionalized Metal–Organic Framework under Dry and Humid Conditions

Robinson W. Flaig,[†] Thomas M. Osborn Popp,[†,⊥] Alejandro M. Fracaroli,[†,‡] Eugene A. Kapustin,[†] Markus J. Kalmutzki,[†] Rashid M. Altamimi,[§] Farhad Fathieh,[†] Jeffrey A. Reimer,[⊥,#] and Omar M. Yaghi*[,†,§]

[†]Department of Chemistry, University of California–Berkeley; Materials Sciences Division, Lawrence Berkeley National Laboratory; Kavli Energy NanoSciences Institute at Berkeley; and Berkeley Global Science Institute, Berkeley, California 94720, United States

[⊥]Department of Chemical and Biomolecular Engineering, University of California–Berkeley, Berkeley, California 94720, United States

[‡]Instituto de Investigaciones en Fisicoquímica de Córdoba, INFIQC–CONICET, Facultad de Ciencias Químicas, Departamento de Química Orgánica, Universidad Nacional de Córdoba, Ciudad Universitaria, X5000HUA Córdoba, Argentina

[§]King Abdulaziz City for Science and Technology (KACST), Riyadh 11442, Saudi Arabia

[#]Materials Sciences Division, Lawrence Berkeley National Laboratory, Berkeley, California 94720, United States

Supporting Information

ABSTRACT: The use of two primary alkylamine functionalities covalently tethered to the linkers of IRMOF-74-III results in a material that can uptake CO_2 at low pressures through a chemisorption mechanism. In contrast to other primary amine-functionalized solid adsorbents that uptake CO_2 primarily as ammonium carbamates, we observe using solid state NMR that the major chemisorption product for this material is carbamic acid. The equilibrium of reaction products also shifts to ammonium carbamate when water vapor is present; a new finding that has impact on control of the chemistry of CO_2 capture in MOF materials and one that highlights the importance of geometric constraints and the mediating role of water within the pores of MOFs.

Metal–organic frameworks (MOFs) are emerging as effective materials for selective CO_2 chemisorption with high uptake due to the ease with which they may be tuned by the pre- and post-synthetic modification of their building units.[1−3] To date, the most successful MOFs for CO_2 capture have included alkylamine-functionalized (R_1NHR_2, or RNH_2) pores. These alkylamines have been shown to selectively react with CO_2, forming covalent C–N bonds, yielding great low-pressure (<100 Torr) uptake and selectivity, yet only ammonium carbamate is reported as the product of CO_2 capture.[4−10] Previously, we demonstrated that the pores of IRMOF-74-III {Mg_2(3,3″-dioxido-[1,1′:4′,1″-terphenyl]-4,4″-dicarboxylate)} can be designed and functionalized with one primary alkylamine covalently attached to each linker leading to enhanced CO_2 capture.[6] Here, we report on a new, diamine-functionalized MOF system, IRMOF-74-III-$(CH_2NH_2)_2$ {Mg_2(2′,5′-bis(aminomethyl)-3,3″-dioxido-[1,1′:4′,1″-terphenyl]-4,4″-dicarboxylate)}, and demonstrate its framework chemistry with CO_2 under dry and humid conditions. This study contributes to the fundamental understanding of CO_2 capture in MOFs under conditions relevant to those required in practice. Although examples of carbamic acid formation in organic molecular crystals, surface modified silica, and porous silica are reported, control of the CO_2-binding chemistry has not been demonstrated.[11−15] We show that the equilibrium of chemisorbed CO_2 shifts at the time when CO_2 is introduced to the system from primarily carbamic acid to ammonium carbamate depending upon the absence or presence of water, respectively. Accordingly, understanding this chemistry is crucial to achieving control over which of the two chemisorption products is formed, as each species' unique properties may make it desirable for specific carbon capture applications.[14,15]

The synthesis and characterization of organic linkers and extended structure, IRMOF-74-III-$(CH_2NH_2)_2$, was carried out according to previously reported conditions [see Supporting Information (SI), Sections S2 and S3].[6] Because the presence of free amines on the organic struts disrupts the synthesis of the extended structure, the two primary amine functional groups were incorporated into IRMOF-74-III as Boc-protected (–Boc = *tert*-butyloxycarbonyl) derivatives.[16] The quantitative removal of the –Boc protecting groups from the framework structure by microwave irradiation (SI, Section S4) was confirmed by solid state cross-polarization magic angle spinning nuclear magnetic resonance spectroscopy (CP-MAS NMR), and Fourier transform infrared spectroscopy (FT-IR), as well as solution phase NMR of the acid-digested material (SI, Sections S5, S6, and S7). Powder X-ray diffraction (PXRD) and nitrogen adsorption isotherm experiments confirmed that the framework maintained its structural integrity and porosity after post-synthetic deprotection of the –Boc groups (SI, Sections S8 and S9).

To confirm that CO_2 binds in a chemisorptive fashion and that it can be removed afterwards, CO_2 isotherms for IRMOF-74-III-$(CH_2NH_2)_2$ were measured at 25 °C (Figure 1). This compound shows similar capacity (67 $cm^3\ g^{-1}$) to the

Received: June 19, 2017
Published: August 17, 2017

DOI: 10.1021/jacs.7b06382
J. Am. Chem. Soc. 2017, 139, 12125–12128

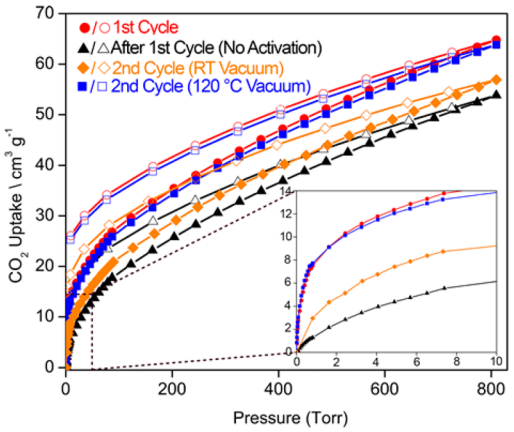

Figure 1. CO_2 isotherms (closed symbols = adsorption; open symbols = desorption) for IRMOF-74-III-$(CH_2NH_2)_2$. In red, after synthesis and activation; in black, after first carbon dioxide isotherm (no activation); in orange, after room temperature activation 12 h; in blue, after 120 °C heating 2 h. (Inset) Expansion of the low pressure range.

previously reported IRMOF-74-III-CH_2NH_2 (75 cm^3 g^{-1}) at 800 Torr, indicating similar physisorption behavior of the materials. In the low pressure range (<100 Torr), however, the IRMOF-74-III-$(CH_2NH_2)_2$ compound significantly out-performs its monoamine counterpart, collecting 2.33 times the amount of CO_2 per gram of material at identical pressures (SI, Section S10), indicative of enhanced chemisorption. The behavior of the material after different activation conditions was also studied (Figure 1). After the first CO_2 isotherm measurement, three separate experiments were conducted: first, a subsequent isotherm was measured without any activation of the material. Investigation of this isotherm reveals a *ca.* 17% drop in CO_2 uptake at 800 Torr, and a *ca.* 83% drop in CO_2 uptake at 0.8 Torr, compared to the as-synthesized, activated material. This suggests that the amine moieties capture the CO_2 by covalent bond formation. The next isotherm was measured after activating the material under dynamic vacuum at 25 °C for 12 h. Investigation of this isotherm reveals a 12% drop in CO_2 uptake at 800 Torr, and a 61% drop in CO_2 uptake at 0.8 Torr. This indicates that only a portion of the amine-CO_2 bonds are broken simply by applying vacuum as shown in Figure 2. Finally, an isotherm was measured after activating the material under vacuum for 2 h at 120 °C. This isotherm showed no drop in CO_2 uptake in both the high and low pressure regions, indicating full regeneration of the material.

The nature of the covalent bond being formed upon CO_2 chemisorption was examined by solid state ^{13}C and ^{15}N CP-MAS NMR of 50% ^{15}N-enriched IRMOF-74-III-$(CH_2NH_2)_2$ (Figure 2). The ^{13}C spectrum (Figure 2a) shows the carbonyl phenoxide peaks at 173 and 166 ppm respectively, as well as the aromatic peaks between 110 and 150 ppm. Of particular note is the CH_2 resonance with two features at 48.6 and 44.0 ppm. Though only one resonance here is expected, this pair of peaks was consistently observed with similar intensity ratios across several tested samples. Likewise, a pair of amine peaks is observed in the ^{15}N spectrum at 30.3 and 25.4 ppm (Figure 2d), where only one amine resonance is expected. These two peaks are surmised to emanate from two distinct conformations of the linkers based on the torsional angle of the central phenyl ring, yielding two distinct amine positions with slightly different chemical shifts. To characterize the chemisorption products of CO_2, samples were exposed to 675 Torr of $^{13}CO_2$ (99% ^{13}C atom basis) in a sealed dosing apparatus for 24 h. (SI, Section S5). The appearance of a highly intense peak in the ^{13}C spectrum (Figure 2b, in red) with a maximum at 160.3 ppm

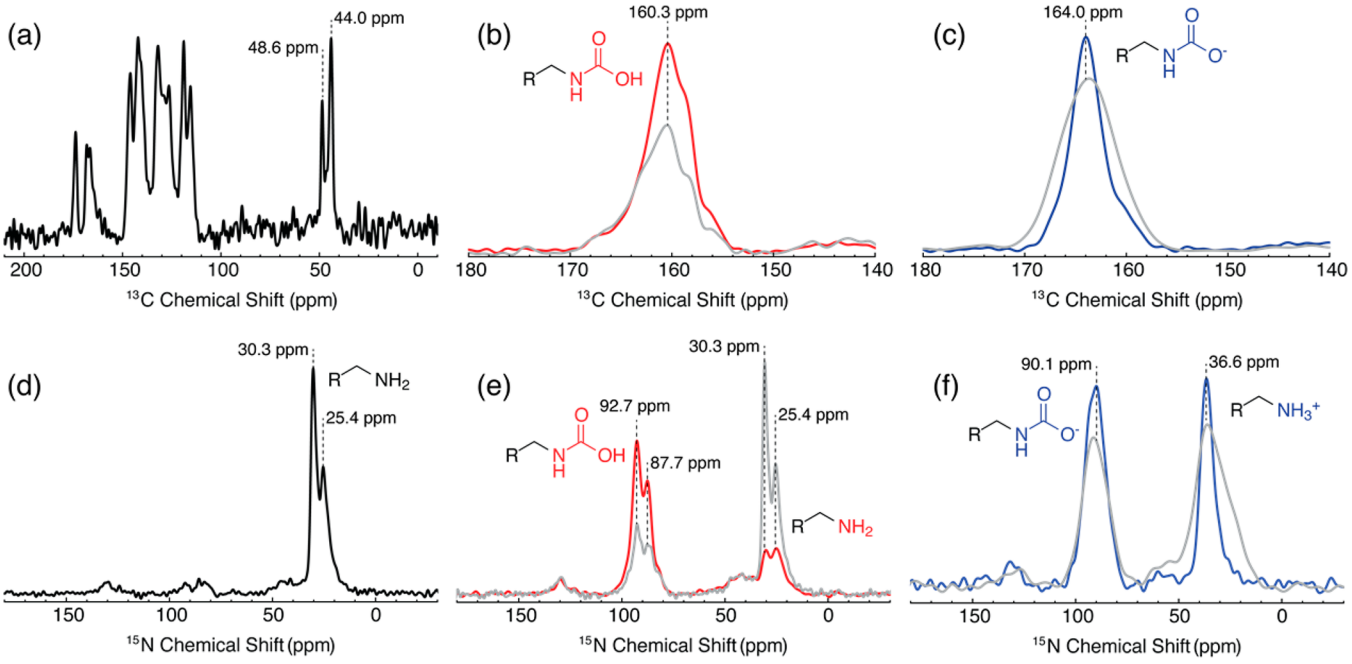

Figure 2. (a) ^{13}C CP-MAS NMR for IRMOF-74-III-$(CH_2NH_2)_2$. (b) ^{13}C CP-MAS NMR after exposure to 675 Torr $^{13}CO_2$ for 24 h (red) and after vacuum for 24 h (gray). (c) ^{13}C CP-MAS NMR after exposure to 95% relative humidity (RH) N_2 atmosphere for 24 h followed by 675 Torr $^{13}CO_2$ for 24 h (blue), and after vacuum for 24 h (gray). (d) ^{15} N CP-MAS NMR for 50% ^{15}N-enriched IRMOF-74-III-$(CH_2NH_2)_2$. (e) ^{15}N CP-MAS NMR after exposure to 675 Torr $^{13}CO_2$ for 24 h (red) and after vacuum for 24 h (gray). (f) ^{15}N CP-MAS NMR after exposure to N_2 atmosphere at 95% RH for 24 h followed by 675 Torr $^{13}CO_2$ for 24 h (blue) and after vacuum for 24 h (gray).

DOI: 10.1021/jacs.7b06382
J. Am. Chem. Soc. 2017, 139, 12125−12128

and right-shoulder features at *ca.* 158 and 156 ppm confirmed that the $^{13}CO_2$ was adsorbed by reaction with the primary amines to form a new species. In contrast to our previous study in which a broad peak spanning 164−160 ppm was assigned to a mixture of carbamate and carbamic acid, this sharp, narrow peak is assigned as primarily carbamic acid. This assertion is consistent with chemical shifts observed and/or calculated for carbamic acid in various structural configurations in other solid CO_2 sorbents.[6,12,14,17] The full width at half-maximum line width of 350 Hz and asymmetric shape of this resonance suggest an inhomogeneous broadening arising from multiple overlapping carbamic acid sites, with each site likely varying slightly in its configuration and hydrogen bonding environment.

Further support of the assignment of this resonance as carbamic acid was gathered via ^{15}N CP-MAS NMR (Figure 2 in red, SI, Section S5). The presence of two residual amine peaks at 30.3 and 25.4 ppm was observed, indicating that complete saturation of the alkylamine moieties was not achieved upon exposure to $^{13}CO_2$ at 675 Torr. Two peaks at 92.7 and 87.7 ppm appear at the expense of the amine peaks, suggesting that this difference in chemical shift, arising from conformations of the linkers, carries over to the chemisorbed products as well. Critically, as no major peak is observed that can be assigned as ammonium, we assign these two downfield peaks as carbamic acid ^{15}N sites. However, when the MOF was exposed to 95% relative humidity (RH) conditions prior to loading with $^{13}CO_2$, a significant new peak at 36.6 ppm is observed along with a peak at 90.1 ppm (Figure 2f, blue). Though these CP-MAS spectra are not quantitative with respect to integration, their similar magnitudes suggest that the species observed here is ammonium carbamate, with the peak at 36.6 ppm being ammonium. The assignment of the adsorbed species as ammonium carbamate is supported by the change in the ^{13}C chemical shift maximum for the 95% RH-treated material to 164.0 ppm (Figure 2c, blue), consistent with previous reports of the ^{13}C chemical shift of carbamate.[12,14,17,18] Though some small portion of this ^{13}C signal may be attributable to bicarbonate, as has been discussed in studies of amine-tethered porous silicas,[18] the ^{15}N spectrum enables us to assert that the dominant amine-CO_2 chemisorption product in humid conditions is ammonium carbamate. The peak splitting observed in the dry adsorption spectrum is lost upon exposure to 95% RH, suggesting that the inter-linker interaction required to produce the ion pair ammonium carbamate alters the torsional angle of the central phenyl ring on the linkers to result in one major structural conformation. This shift to ammonium carbamate from carbamic acid occurs as a function of the amount of water vapor present, with MOF samples exposed to atmospheric moisture (50% RH) exhibiting signal contributions from both carbamic acid and carbamate (SI, Section S5).

Although the role of water is critical to this chemistry, initial examination in modeled IRMOF-74-III-$(CH_2NH_2)_2$ of the separation between primary amines points to geometric constraints within the pores as also being operative. To further understand the amine−amine distances and their contribution to this unique chemistry, we modeled the conformation of the linkers (Figure 3, SI Section S11) in IRMOF-74-III-$(CH_2NH_2)_2$. Because the amines are introduced to the material as their −Boc protected counterparts, steric hindrance plays a significant role in their final orientation. When considering amine geometries that would facilitate formation of carbamic acids, two possible intermethylene distances (staggered amine

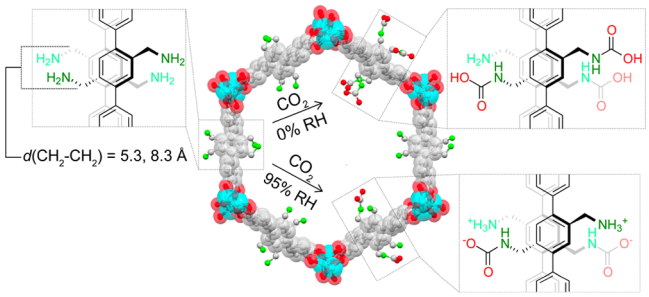

Figure 3. View of modeled IRMOF-74-III-$(CH_2NH_2)_2$ [staggered amine] structure down the crystallographic *c*-axis, depicting the three possible pore environments before (left pore wall) and after exposure to CO_2 under 95% RH (bottom right pore wall) and dry (upper right pore wall) conditions. Dashed boxes clarify the chemisorbed species upon reaction between linker-based alkylamine and CO_2 under the respective conditions. H atoms are omitted for clarity. Color code: C, gray; O, red; N, green; and Mg, blue.

conformation), 5.3 and 8.3 Å, were of particular interest since similar intermethylene distances have been found in molecular carbamic acids (5.982(4) Å, and 8.017(1) Å).[11,15] The similarities between these distances and those in IRMOF-74-III-$(CH_2NH_2)_2$ support the notion of carbamic acid formation in the absence of a proton-transfer species (in the present case, water) which would generate ammonium carbamate.

For additional experimental support of these two species, FT-IR (SI, Section S6), combined thermogravimetric analysis, differential scanning calorimetry, mass spectrometry (TGA-DSC-MS, SI Section S12), and breakthrough measurements (SI, Section S13) were performed. Samples of IRMOF-74-III-$(CH_2NH_2)_2$, exposed to CO_2 were also analyzed using TGA-DSC-MS. The sample lost 12 mass % of CO_2 (m/z = 44) at relatively low temperature (onset at 47 °C) after exposure to dry CO_2. Humidified (95% RH) samples of IRMOF-74-III-$(CH_2NH_2)_2$ that were exposed to CO_2 exhibit a mass loss of 10 mass % corresponding to CO_2 (m/z = 44) and H_2O (m/z = 18) at higher temperature (onset at 65 °C). The results of the thermal analysis indicate CO_2 is more strongly bound as ammonium carbamate as opposed to carbamic acid under wet and dry conditions, respectively. Additionally, the decrease in mass loss under humid conditions supports the conclusion of two amines participating in ammonium carbamate formation versus one amine forming carbamic acid upon reaction with CO_2. The dynamic adsorption capacity, as measured by breakthrough time, remained the same under dry (900 ± 10 s g^{-1}, 1.2 mmol g^{-1}) and 65% RH (890 ± 10 s g^{-1}, 1.2 mmol g^{-1}) conditions (SI, Section S13). This appears counterintuitive given the TGA-DSC-MS results, but is justified by the fact that at 50% RH (SI, Section S5) we observe a mixture of carbamate and carbamic acid in the solid state NMR. This mixture would likely be the result of initial carbamic acid generation, with subsequent proton transfer to form ammonium carbamates, and thus the kinetics of CO_2 capture would be dictated by the formation of the former species.

To investigate the difference in thermal properties between ammonium carbamate and carbamic acid in IRMOF-74-III-$(CH_2NH_2)_2$ and their impact on regeneration of the material, vacuum was applied for 24 h at room temperature to the NMR samples previously exposed to $^{13}CO_2$, and solid state CP-MAS NMR was performed. Under dry loading conditions, the ^{13}C carbamic acid resonance at 160.3 ppm is significantly reduced after vacuum (Figure 2b, gray), and the ^{15}N carbamic acid

DOI: 10.1021/jacs.7b06382
J. Am. Chem. Soc. 2017, 139, 12125−12128

resonances at 92.7 and 87.7 ppm decrease as the two amine peaks at 30.3 and 25.4 ppm rise in intensity (Figure 2e, gray). For the sample exposed to both 95% RH and $^{13}CO_2$, room temperature vacuum activation appears much less effective (Figure 2c,f), with only minor loss of signal observed for the carbamate resonance in both the ^{13}C and ^{15}N spectra. This is consistent with the TGA-DSC-MS results, where the onset point of CO_2 desorption as carbamate occurs 18 °C higher than for carbamic acid.

■ ASSOCIATED CONTENT

Supporting Information

The Supporting Information is available free of charge on the ACS Publications website at DOI: 10.1021/jacs.7b06382.

Methods and additional data (PDF)

■ AUTHOR INFORMATION

Corresponding Author

*yaghi@berkeley.edu

ORCID

Robinson W. Flaig: 0000-0003-3090-4724
Alejandro M. Fracaroli: 0000-0003-3016-6813
Eugene A. Kapustin: 0000-0003-4095-9729
Omar M. Yaghi: 0000-0002-5611-3325

Notes

The authors declare no competing financial interest.

■ ACKNOWLEDGMENTS

This work was supported as part of the Center for Gas Separations Relevant to Clean Energy Technologies, an Energy Frontier Research Center funded by the U.S. Department of Energy, Office of Science, Basic Energy Sciences under Award # DE-SC0001015 (CO_2 uptake and NMR studies). We also acknowledge BASF (Ludwigshafen, Germany) for support toward synthesis. R.W.F and T.M.O.P. acknowledge funding from the NSF Graduate Fellowship Research Program. We are also very grateful to Mr. Kyle E. Cordova, Mr. Peter J. Waller, and Dr. Hiroyasu Furukawa for helpful discussions. M.J.K. is grateful for financial support through the German Research Foundation (DFG, KA 4484/1-1).

■ REFERENCES

(1) Cohen, S. M. *Chem. Rev.* **2012**, *112*, 970.
(2) Belmabkhout, Y.; Guillerm, V.; Eddaoudi, M. *Chem. Eng. J.* **2016**, *296*, 386.
(3) Schoedel, A.; Ji, Z.; Yaghi, O. M. *Nat. Energy* **2016**, *1*, 16034.
(4) McDonald, T. M.; D'Alessandro, D. M.; Krishna, R.; Long, J. R. *Chem. Sci.* **2011**, *2*, 2022.
(5) Planas, N.; Dzubak, A. L.; Poloni, R.; Lin, L.-C.; McManus, A.; McDonald, T. M.; Neaton, J. B.; Long, J. R.; Smit, B.; Gagliardi, L. *J. Am. Chem. Soc.* **2013**, *135*, 7402.
(6) Fracaroli, A. M.; Furukawa, H.; Suzuki, M.; Dodd, M.; Okajima, S.; Gándara, F.; Reimer, J. A.; Yaghi, O. M. *J. Am. Chem. Soc.* **2014**, *136*, 8863.
(7) Li, L.-J.; Liao, P.-Q.; He, C.-T.; Wei, Y.-S.; Zhou, H.-L.; Lin, J.-M.; Li, X.-Y.; Zhang, J.-P. *J. Mater. Chem. A* **2015**, *3*, 21849.
(8) McDonald, T. M.; Mason, J. A.; Kong, X.; Bloch, E. D.; Gygi, D.; Dani, A.; Crocellà, V.; Giordanino, F.; Odoh, S. O.; Drisdell, W. S.; Vlaisavljevich, B.; Dzubak, A. L.; Poloni, R.; Schnell, S. K.; Planas, N.; Lee, K.; Pascal, T.; Wan, L. F.; Prendergast, D.; Neaton, J. B.; Smit, B.; Kortright, J. B.; Gagliardi, L.; Bordiga, S.; Reimer, J. A.; Long, J. R. *Nature* **2015**, *519*, 303.
(9) Liao, P.; Chen, X.; Liu, S.; Li, X.; Xu, Y.; Tang, M.; Rui, Z.; Ji, H.; Zhang, J.; Chen, X. *Chem. Sci.* **2016**, *7*, 6528.
(10) Gómora-Figueroa, A. P.; Mason, J. A.; Gonzalez, M. I.; Bloch, E. D.; Meihaus, K. R. *Inorg. Chem.* **2017**, *56*, 4308.
(11) Aresta, M.; Ballivet-Tkatchenko, D.; Dell'Amico, D. B.; Boschi, D.; Calderazzo, F.; Labella, L.; Bonnet, M. C.; Faure, R.; Marchetti, F. *Chem. Commun.* **2000**, *8*, 1099.
(12) Pinto, M. L.; Mafra, L.; Guil, J. M.; Pires, J.; Rocha. *Chem. Mater.* **2011**, *23*, 1387.
(13) Switzer, J. R.; Ethier, A. L.; Flack, K. M.; Biddinger, E. J.; Gelbaum, L.; Pollet, P.; Eckert, C. A.; Liotta, C. L. *Ind. Eng. Chem. Res.* **2013**, *52*, 13159.
(14) Mafra, L.; Čendak, T.; Schneider, S.; Wiper, P. V.; Pires, J.; Gomes, J. R. B.; Pinto, M. L. *J. Am. Chem. Soc.* **2017**, *139*, 389.
(15) Inagaki, F.; Matsumoto, C.; Iwata, T.; Mukai, C. *J. Am. Chem. Soc.* **2017**, *139*, 4639.
(16) Lun, D. J.; Waterhouse, G. I. N.; Telfer, S. G. *J. Am. Chem. Soc.* **2011**, *133*, 5806.
(17) Li, D.; Furukawa, H.; Deng, H.; Liu, C.; Yaghi, O. M.; Eisenberg, D. S. *Proc. Natl. Acad. Sci. U. S. A.* **2014**, *111*, 191.
(18) Chen, C.; Shimon, D.; Lee, J. J.; Didas, S. A.; Mehta, A. K.; Sievers, C.; Jones, C. W.; Hayes, S. E. *Environ. Sci. Technol.* **2017**, *51*, 6553.

DOI: 10.1021/jacs.7b06382
J. Am. Chem. Soc. 2017, 139, 12125−12128